ELSEVIER

Contents lists available at ScienceDirect

Journal of Materials Science & Technology

journal homepage: www.elsevier.com/locate/jmst



Review Article

Advanced high-entropy alloys breaking the property limits of current materials



Dongyue Li^{a,*}, Peter K. Liaw^b, Lu Xie^a, Yong Zhang^c, Wenrui Wang^{a,*}

- ^a School of Mechanical Engineering, University of Science and Technology Beijing, Beijing 100083, China
- ^b Department of Materials Science and Engineering, The University of Tennessee, Knoxville, TN 37996, USA
- ^c Beijing Advanced Innovation Center of Materials Genome Engineering, State Key Laboratory for Advanced Metals and Materials, University of Science and Technology Beijing, Beijing 100083, China

ARTICLE INFO

Article history:
Received 21 September 2023
Revised 28 November 2023
Accepted 3 December 2023
Available online 6 January 2024

Key words:
High-entropy alloy
Strength-ductility
Trade-off
Microstructure
Deformation mechanism

ABSTRACT

The growing need for stronger and more ductile structural materials has spurred an intense search for innovative, high-performance alloys. Traditionally, alloys face a pervasive trade-off: high strength often comes at the expense of ductility and vice versa. The advent of high-entropy alloys (HEAs) offering both high strength and ductility has transformed this landscape. In this work, we discuss the deformation mechanisms of HEAs, examine the foundations of the strength-ductility trade-off, and explore approaches for designing HEAs to surmount this limitation. Furthermore, we analyze the factors that govern HEA-deformation performance, which in turn influence the HEA design. We also propose a perspective on future research directions concerning the mechanical behavior of HEAs, highlighting potential breakthroughs and novel strategies to advance the field.

© 2024 Published by Elsevier Ltd on behalf of The editorial office of Journal of Materials Science & Technology.

1. Introduction

The concept of the "trade-off" stems from limitations of many origins. It is often used to describe situations in everyday life and is widely-regarded as central to the foundation of the improvement in many aspects [1,2]. Developing advanced materials with a substantial improvement in both strength and ductility is our goal. However, many strategies that effectively strengthen materials sacrifice ductility, resulting in the so-called strength-ductility trade-off [3,4]. The trade-off between strength, i.e., the ability to withstand applied stress and ductility, the capability to undergo significant plastic deformation, hampers the performance and applicability of structural materials [5].

In recent years, exciting breakthroughs have led to novel strategies that successfully achieve decent tensile ductility while maintaining strength [6–8]. These strategies can be categorized into component design, structural design and post-processing methods. In fact, compared with conventional materials, the design concept of HEAs offers more room for microstructural manipulation and optimization [9–13]. These approaches led to unprecedented high strength-ductility combinations and original deformation mecha-

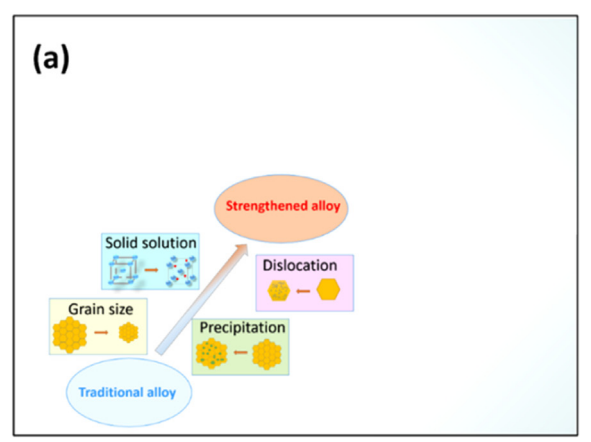
E-mail addresses: lidongyue@ustb.edu.cn (D. Li), gmbitwrw@ustb.edu.cn (W. Wang).

nisms. For instance, the addition of Si to CoCrFeNi enhances yield strength, ultimate strength, and ductility, attributed to a synergistic effect of improved solid solution strengthening and reduced stacking fault energy [14]. Reducing the valence electron number has also been explored and demonstrated in achieving the desired properties [15,16].

From the perspective of structural design, nano-twinned microstructure has been utilized to overcome the strength-ductility trade-off in copper [17]. Generally, nanostructured metals are strong because ultrahigh density internal boundaries restrict the mean free path of dislocations. But they are also more brittle due to the diminished work-hardening ability. Nano-twinned metals/alloys with coherent interfaces of mirror symmetry can overcome this inherent trade-off [18]. Strengthening occurs through twin boundaries interacting with dislocations and losing their cohesiveness during plastic deformation [19]. These findings have provided valuable insights into the development of advanced materials.

Moreover, significant progress has been made in enhancing the strength and slightly reducing the ductility of HEAs through post-processing methods, such as cold rolling and annealing [20–22]. The interphase strengthening effects contribute to the superior mechanical performance of multiphase HEAs at the micro/nano scale, surpassing that of single-phase HEAs [23]. Other approaches, including introducing twin boundaries and gradient grain sizes

^{*} Corresponding authors.



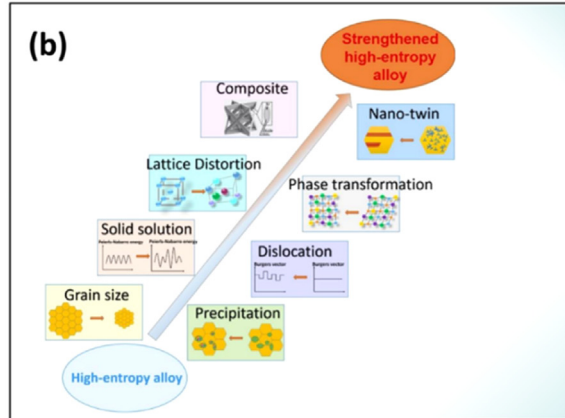


Fig. 1. Toughening mechanisms of (a) traditional alloys and (b) HEAs.

[24], controlling the size, morphology, and distribution of secondary phases [25–29], have been explored and demonstrated to varying extents in achieving this desired goal.

HEAs are novel and versatile alloys with attractive mechanical properties [30-37]. These approaches led to unprecedented high strength-ductility combinations and original deformation mechanisms. However, the strength-ductility trade-off has also been a long-standing dilemma in HEAs, which has been one of the key factors restricting their potential applications as a new class of structural materials [12,38-42]. For instance, single-phase facecentered-cubic (FCC) HEAs typically exhibit high ductility but low ultimate tensile strengths at room temperature [34,43]. Bodycentered-cubic (BCC) HEAs generally fracture due to early cracking, with limited plasticity at room temperature, restricting their malleability and widespread use [33,44]. Recent works also addressed HEAs with single hexagonal-close-packed (HCP) structures, such as YGdTbDyHo, YGdTbDyLu, or GdTbDyTmLu alloys [45-49]. Most of the HCP HEAs consist of heavy rare-earth elements. Nevertheless, a number of studies about HCP HEAs focus on the compositions and phase structures, and their mechanical properties are yet scarce.

Overcoming the strength-ductility trade-off is a key challenge in the development of HEAs. The purpose of this paper is to review the advances made in attempts to break this barrier and discuss several strategies that form the foundation of our understanding of the improvement process.

2. Mechanisms for overcoming strength-ductility trade-off

Compared to the classical alloy-strengthening mechanisms of alloys, i.e., solid-solution strengthening, fine-grain strengthening, precipitation strengthening, dislocation strengthening, etc. [19,50], HEAs display original and unique toughening mechanisms [33,51]. Meanwhile, the conventional deformation mechanisms have variations due to the unique structures of HEAs, as exhibited in Fig. 1. For instance, the severe lattice distortion is a core effect of HEAs, which enhances the lattice friction stress experienced by dislocations and increases the sensitivity of the yield stress on grain size. The second phase in the precipitation-strengthening mechanism of HEAs is not a simple phase structure but a high-entropy precipitation phase, i.e., multicomponent intermetallic nano-particles [52], spinodal order-disorder nano-precipitates [26], or ordered oxygen complexes [53], etc. Moreover, the Peierls-Nabarro energy barrier is periodic in a dilute solid solution, while the distortions in the lattice and Peierls-Nabarro energy are variational for HEAs [34]. Besides, the Burgers vector of the dislocation in HEAs is not a fixed value as well. Thus, HEAs are stronger than traditional alloys during deformation. This phenomenon can be even extended

to the phase-transformation process [54,55]. More energy is absorbed during the phase transformation due to the severe lattice distortion. Furthermore, the nano-twinning mechanism in HEAs can be activated at cryogenic temperatures, which simultaneously increases the strength and toughness of HEAs [56–62]. With the development of HEAs, composites have become a new means of increasing strength and ductility at once [63]. The detailed mechanisms of HEAs to overcome the strength-ductility trade-off are described as follows.

2.1. Precipitation

In fact, precipitation hardening is the most potent strengthening method for many alloys [25,64,65]. Second-phase intermetallic compounds provide an efficient approach for enhancing alloy strengths. In the same way, precipitation strengthening is a promising approach for HEAs to overcome the strength-ductility trade-off [66–69].

Generally, precipitates evenly distributed in the grains of the matrix produce a strong barrier to dislocation motion [70]. There are two possible ways to overcome such obstacles, the by-pass mechanism (Orowan-type) and particle-shearing mechanism [71]. The strength of the obstacle, the distance between the obstacles, and the elastic stiffness of the material are the main factors in determining the mechanism of overcoming obstacles [25,72].

The Orowan mechanism occurs when the radius of particles exceeds a critical value or is incoherent with the matrix. The strength increment for the Orowan bypass mechanism $(\Delta \sigma_0)$ is given by Eq. (1):

$$\Delta\sigma_0 = \frac{0.4M}{\pi} \frac{Gb}{\sqrt{1-\nu}} \frac{\ln\left(\sqrt[2]{\frac{2}{3}} \cdot \frac{r}{b}\right)}{\lambda} \tag{1}$$

where M is the Taylor factor, G is the shear modulus, r is the precipitate radius, b is the Burgers vector, and λ is the wavelength of the Cu $K\alpha$ radiation.

When precipitates are sufficiently small and coherent with the matrix, the shearing mechanism would dominate the interaction between dislocations and precipitates. First, the contribution to the yield strength from atomic-order strengthening ($\Delta\sigma_{\rm os}$) is given by Eq. (2):

$$\Delta\sigma_{\rm os} = 0.81 M \frac{\gamma_{\rm APB}}{2b} \cdot \left(\frac{3\pi\,\varphi}{8}\right)^{\frac{1}{2}} \tag{2}$$

where $\gamma_{\rm APB}$ is the anti-phase boundary energy of the precipitates, and φ is the volume fraction of the precipitates.

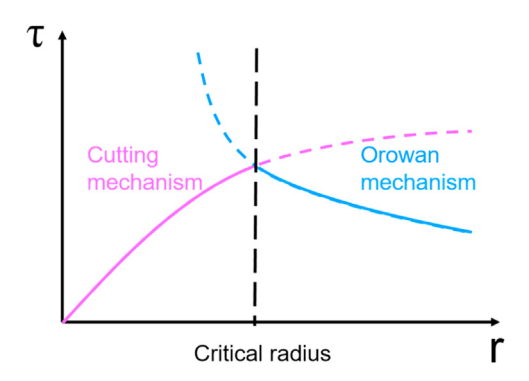


Fig. 2. Dependence of the strengthening effect on the radii of precipitates.

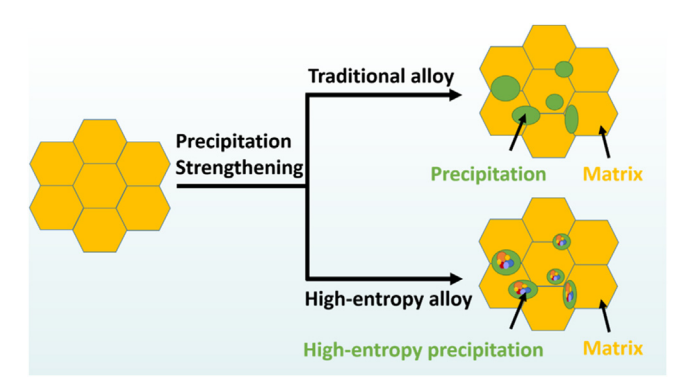


Fig. 3. Schematic diagram of the difference in precipitation strengthening between traditional alloys and HEAs.

The increase in yield strength due to coherency strengthening is given by Eq. (3):

$$\Delta \sigma_{\rm cs} = M\alpha_{\varepsilon} (G\varepsilon)^{\frac{3}{2}} \cdot \left(\frac{r\varphi}{0.5Gb}\right)^{\frac{1}{2}} \tag{3}$$

where α_{ε} is a constant, and ε is the constrained lattice-parameter mismatch.

Strengthening by the modulus mismatch is given by Eq. (4):

$$\Delta\sigma_{\rm ms} = 0.0055 M (\Delta G)^{\frac{3}{2}} \cdot \left(\frac{2\varphi}{Gb^2}\right)^{\frac{1}{2}} \cdot b \left(\frac{r}{b}\right)^{\left(\frac{3m}{2}-1\right)} \tag{4}$$

where ΔG is the shear-modulus mismatch between the matrix and the precipitates, and m is a constant.

If we keep the volume fraction of the particles constant, the result is a curve that increases proportionally to the square root of the particle radius and reaches a maximum beyond which the curve drops again. The particle radius is optimal at the intersection of the two curves i.e., the contribution to strengthening is maximized (Fig. 2).

The most obvious difference of precipitate strengthening between traditional and high-entropy alloys is that the precipitates are more complex and concentrated, i.e., high-entropy precipitates, which lead to better strengthening effects (Fig. 3) [65,73,74].

Additionally, the sluggish diffusion effect in HEAs provides favorable conditions for forming more stable and fine nano-sized precipitates and helps control the precipitate size [75]. The sluggish diffusion effect reduces the migration rate of elements in the solid state, leading to the formation of smaller and more uniformly distributed precipitates. These fine nano-sized precipitates can effectively enhance the material's strength and fatigue resistance while maintaining good ductility [75,76]. Nevertheless, whether HEAs have slower diffusion, relative to conventional alloys, is still a subject of further study, which may be dependent upon the composition [33,77].

For instance, Yang et al. [52] demonstrated a strategy to break this trade-off by controllably introducing high-density ductile multicomponent intermetallic nano-particles in (FeCoNi)₈₆-Al₇Ti₇ HEAs. Typical microstructural features with an elemental partition between the matrix and multicomponent intermetallic nano-particles were observed. The (FeCoNi)₈₆-Al₇Ti₇ alloy exhibits a strength of 1.5 GPa and ductility of 50 % in tension, which was compared with other alloys at room temperature. This property can be eliminated by generating a distinctive multistage work-hardening behavior, resulting from pronounced dislocation activities and deformation-induced micro-bands.

Liang et al. [26] aimed to obtain a final microstructure combining a near-equiatomic matrix with high-content ductile precipitates, regardless of the initial atomic ratio. HEAs with high-content nano-precipitates were obtained by phase separation. The spinodal decomposition creates a low-misfit coherent nano-structure combining the disordered FCC matrix with high-content ductile ordered nano-precipitates. The spinodal order-disorder nano-structure contributes to a strength increase of \sim 1.5 GPa (> 560 %), relative to the HEA without precipitation, achieving 1.9 GPa while retaining good ductility (> 9 %). The result is significant dislocation storage required for compatible plastic strains, allowing a high strain-hardening rate that leads to larger uniform strains while elevating strengths.

Besides adding different metal elements in HEAs, the addition of small non-metallic atoms has also brought surprising changes to the mechanical behavior. The anomalous interstitial-strengthening behavior of the (TiZrHfNb)₉₈O₂ is better with respect to a number of developed alloys [53]. The mechanical properties of the current TiZrHfNb have strong dependence on the specific concentration of oxygen. This type of ordered interstitial complex strengthening mechanism is a new type of strain-hardening mechanism based on ordered interstitial complexes. It enables balance among the dislocation pinning, multiplication, and substructure homogenization, thereby leading to a high strain-hardening rate and an increase in both strength and ductility [53].

Moreover, heavy carbon-alloyed HEAs could possess a supreme combination of high tensile strength (935 MPa) and great ductility (\sim 74 %) [78]. The excellent mechanical properties were ascribed to that carbon atoms suppress the dislocation motion and promote the deformation-induced twinning. Simultaneously, the ductility is further secured for the single FCC structure maintained due to appropriate carbon alloying. Seol et al. [79] found that boron doping in FeMnCrCoNi and Fe $_{40}$ Mn $_{40}$ Cr $_{10}$ Co $_{10}$ (atomic percent, at. %) dramatically improves their mechanical properties. Boron decorates the grain boundaries and acts twofold, through interface strengthening and grain-size reduction. These effects enhance the grain-boundary cohesion and retard capillary-driven grain coarsening, thereby qualifying boron-induced grain-boundary engineering as an ideal strategy for the development of advanced HEAs.

2.2. Stacking fault energy

Tuning stacking fault energy (SFE) through alloying stands as a robust protocol for manipulating the deformation mechanism and subsequent mechanical properties of metallic materials. SFE is a parameter finely adjusted through alloy composition. It significantly dictates diverse dislocation behaviors. The reduction of SFE is widely acknowledged to promote dislocation dissociation and deformation twinning while inhibiting cross-slip. These alterations notably augment the work-hardening capabilities of materials, thereby enhancing their mechanical properties. Hence, the strategic tuning of SFE via compositional design emerges as one of the most effective strategies for achieving superior mechanical properties across various metallic material systems, including steels, HEAS, Cu alloys, and Ti alloys [80]. The marked enhance-

ment in mechanical performance primarily originates from the activation of twinning-induced plasticity or transformation-induced plasticity. Both of them are fundamentally rooted in the meticulous modification of SFE.

Research delineated a notable decrease in the sample size effect on strength with diminishing SFE. Understanding the interplay between SFE and mechanical properties in HEAs is a crucial pursuit across a spectrum of studies. Investigation into nanostructured alloys processed via high-pressure torsion revealed an intriguing trend: reduced SFE aligns with heightened strength, particularly evident in alloys with lower aluminum content. However, at extremely reduced grain sizes, this correlation between SFE and strength appears to reverse, impacting material uniform elongation [81].

Exploration of CrCoNi alloys uncovered a unique deformation mechanism, which is dual phase transformations intertwined with continuous shear. This arises from the alloy's capacity to facilitate flexible stacking sequences of low SFE layers, thereby enabling unconventional deformation mechanisms [82]. Investigations into Cantor HEAs of CrMnFeCoNi showed deformation-induced crystalline-to-amorphous phase transformations. These transformations enhance toughening mechanisms within the alloy structure. They increase crack-tip dislocation densities and form an amorphous phase, presenting a new way to improve material toughness [83].

Further exploration into cryogenic-deformation-induced phase transformations in FeCoCrNi HEAs emphasized the significance of temperature-dependent phase stability [84]. Despite theoretical predictions favoring phase transformation due to lower free energy, kinetic limitations impact the occurrence of these transformations, highlighting the complexity of phase transitions in these alloys. Theoretical investigations into transformationmediated twinning mechanisms unveiled a two-step phase transformation process influenced by negative SFE in metastable FCC materials [85]. However, challenges persist in experimentally determining SFE in metastable alloys, underscoring discrepancies between calculated and experimental values. This underscores the critical need for refined methodologies to precisely measure SFE in these materials [80,86]. This comprehensive body of research underscores the profound influence of SFE on deformation mechanisms and mechanical properties in HEAs, emphasizing the necessity for more precise and reliable measurement techniques in this domain.

2.3. Short range order

In principle, it is generally believed that HEAs maintain stable single-phase disordered solid solution states, due to their highentropy effect. For example, the results of the Cantor alloy microstructure analysis show that the atomic arrangement in HEAs reaches almost ideal random mixing conditions. However, with the development of research, it is now believed that the arrangement of atoms in high-entropy alloys is not an ideal disorder state, and the coexistence of short range order (SRO) or multiphases is common [87–89]. The schematic diagram is shown in Fig. 4.

Although there are lots of propositions that the SRO could tune the deformation mechanisms and then mechanical properties, direct experimental evidence is still lacking. Measuring SRO in HEAs is crucial for understanding their properties and underlying atomic interactions [90]. Several experimental techniques can be employed to investigate SRO in HEAs, including high-resolution synchrotron X-ray diffraction (XRD) [91], neutron scattering [88], electron microscopy [92], and atom probe tomography (APT) [93]. XRD and neutron scattering are powerful methods for probing atomic arrangements in crystalline materials, while electron microscopy techniques like high-resolution transmission electron mi-

croscopy (HRTEM) and scanning transmission electron microscopy (STEM) allow for direct visualization of atomic arrangements at the nanometer scale. APT, on the other hand, provides 3D atomic-scale compositional information, which can be used to analyze the distribution of elements and the presence of short-range order in the alloy.

Recently, Niu et al. [94] utilized in-situ TEM to investigate deformation mechanisms in alloys with high SRO. Their findings offer intriguing insights, providing valuable information for the ongoing exploration of the role of SRO in deformation mechanisms and the resulting mechanical properties. The influence of SRO partially inhibits the formation of deformation twins in the alloy, leading to the predominance of localized slip as the primary plastic deformation mechanism. This effect, combined with other factors in the alloy, such as SFE, collectively shapes the material's deformation behavior.

In addition to experimental methods, computational techniques such as molecular dynamics (MD) simulations [95] and density functional theory (DFT) calculations [96] can be used to simulate atomic structures and interactions in HEAs. These methods help obtain atomic-scale information about the alloy's structure and predict the presence of short-range order under various conditions. To gain a comprehensive understanding of SRO in high-entropy alloys, it is advisable to use a combination of these techniques. Comparing experimental and computational results enables a more accurate assessment of the short-range order and its influence on the properties of the alloy.

From the perspective of the atomic group, Ma et al. [87] believed that in high-entropy alloys, the strengthening effects of atoms not only exist independently but also converge together to provide strengthening effects. The distribution of atoms in highentropy alloys is highly concentrated, and the interaction between atoms through electrons in high-entropy alloys cannot be ignored. The interaction between electrons affects the atomic size and the enthalpy of mixing, resulting in a heterogeneous composition in high-entropy alloys.

Wu et al. [88] proposed that the SRO structure is a chemical or topological configuration that deviates from the disordered atoms within a few atomic scales. It is similar to the nano-scale precipitated phase but does not have the typical characteristics of a precipitated phase. Therefore, the ordered group of atoms can be regarded as the precursor before precipitate formation or the cluster obtained by precipitate decomposition.

The SRO structure is generally not the only strengthening mechanism of HEAs, but it plays a role in coordinating various strengthening and toughening mechanisms. It is possible to introduce SRO structures into various interfaces to further enhance their impact on the toughening mechanism. However, whether SRO affects the strength of HEAs is still a subject of further study [97,98].

2.4. Severe lattice distortion

It is demonstrated that severe lattice distortion improves both the yield stress and its sensitivity to grain size [99–103]. Different atoms elastically distort the crystal, and the elastic distortion of the lattice interacts with that around the dislocation. For instance, if the atoms are larger than the surrounding atoms, they produce compressive stress in the vicinity. When the dislocations attempt to enter the compressive region, they will be excluded and require additional energy to move on. If the dislocations approach the atoms with the stretched region, they will be attracted. Thus, it becomes difficult to detach the dislocation from the atom, pinning the dislocation. Smaller atoms behave the opposite.

One major distinction between traditional and HEAs is the concentration of solute atoms in a solid solution [104,105]. Traditional alloys have limited solubility due to their large radius difference.

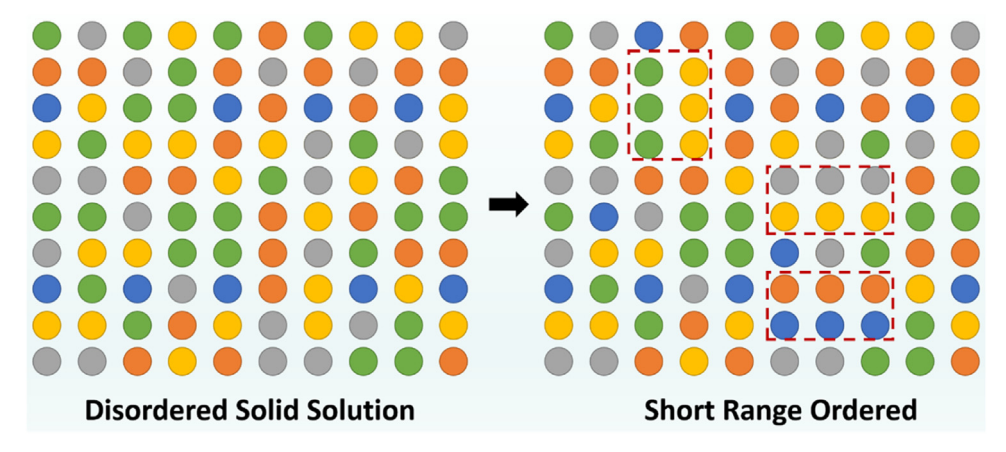


Fig. 4. Schematic illustration of the formation of SRO structures in disordered solid solutions of HEAs.

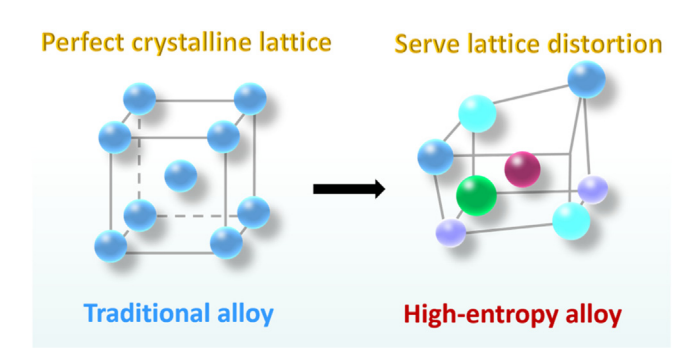


Fig. 5. Schematic diagram of the difference in crystal structures between traditional alloys and HEAs.

Thus, they usually achieve only moderate strengthening. However, HEAs involve multiple solutes and become difficult to identify a "solvent", such as the so-called complex concentrated alloys [106–108]. The degree of the solid solution of HEAs has reached a maximum. Experimentally, the following relation between the contribution to strengthening, $\sigma_{\rm ss}$, and the concentration, c, of the solvent atoms is found by Eq. (5):

$$\Delta \sigma_{\rm ss} \propto c^n$$
 (5)

The exponent, *n*, takes values of about 0.5. From the equation, we might infer that HEAs choosing atoms with differing radii as substitutional atoms will achieve a larger strengthening contribution than traditional alloys. Fig. 5 illustrates this trend, using the sphere model of atoms.

Sohn et al. [109] have shown that the VCoNi equiatomic medium-entropy alloy exhibits a near 1 GPa yield strength and good ductility, outperforming conventional solid-solution alloys. Furthermore, the dislocation-mediated plasticity effectively enhances the strength-ductility relationship by generating nano-sized dislocation substructures due to massive pinning. The lattice-friction stress is expressed by the following Eq. (6):

$$\sigma_0 = 2MG/(1 - \nu)\exp(-2\pi w/b) \tag{6}$$

where M=3.06 is the Taylor factor for the FCC phase, G is the shear modulus, v is the Poisson's ratio, w is the width of a dislocation, and b is the magnitude of the Burgers vector. The results demonstrate that severe lattice distortion is one of the key properties for identifying strong materials for structural engineering applications.

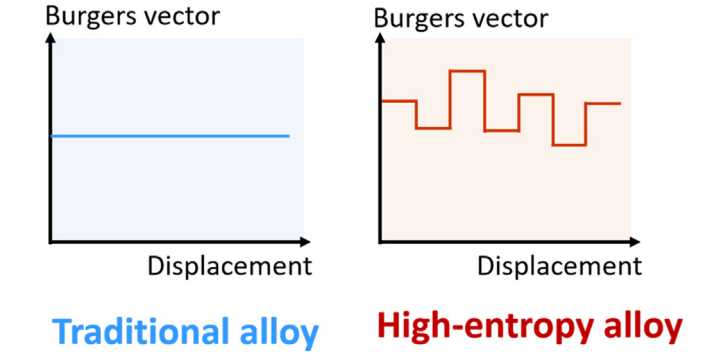


Fig. 6. Schematic diagram of the burgers vector in dislocation strengthening between traditional alloys and HEAs.

2.5. Dislocations

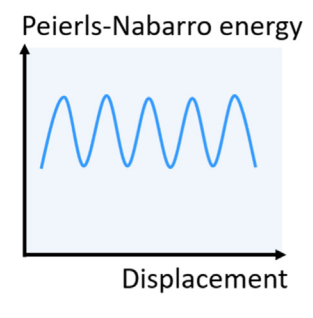
The yield strengths of alloys derive from the lattice resistance to dislocation motion [3]. Dislocations are one-dimensional lattice defects, which tend to increase the material strength [42,110,111]. A higher dislocation density may induce an increase in strength. If a sufficiently large shear stress acts on a dislocation, the dislocation moves through the crystal. There are two vectors that can describe an edge dislocation: One is the line vector, t, pointing the direction; another is the Burgers vector, b, which can be determined by the Burgers circuit around the dislocation line [112].

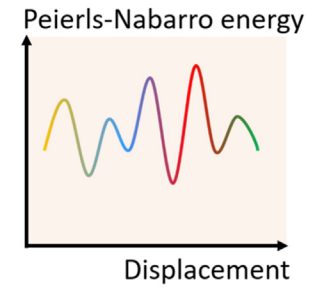
In contrast to traditional alloys, where the Burgers vector is constant due to the stable distance of atoms, the Burgers vector in HEAs constantly varies because the environment around each atom is diverse, as visualized in Fig. 6. The role of the configurational entropy, the influence of multiple principal elements on the dislocation core structure, and the interaction between dislocations and various types of defects or solute atoms contribute to the unique dislocation-strengthening mechanisms in HEAs.

Deng et al. [113] observed that high-density active dislocations in $Fe_{40}Mn_{40}Co_{10}Cr_{10}$ HEAs overlapped and crisscrossed with each other, resulting in a high-density dislocation wall and hindering the movement of the dislocation. At high strains, deformation twinning is activated as an additional mechanism leading to strain hardening. The dislocation-strengthening value can be calculated according to Eq. (7)

$$\Delta \sigma_{\rm dis} = M\alpha Gb \rho^{1/2} \tag{7}$$

where $\Delta \sigma_{
m dis}$ represents the dislocation-strengthening value, M and lpha are 3.06 and 0.2 for a face-centered-cubic phase, respec-





Traditional alloy

High-entropy alloy

Fig. 7. Schematic diagram of the Peierls-Nabarro energy in dislocation strengthening between traditional alloys and HEAs.

tively, G represents the shear modulus, b represents the Burgers vector, and ρ represents the density.

The atomic bonds have to flip for a dislocation to move, which requires stretching. The resulting Peierls-Nabarro force fixes the dislocation at its momentary position and has to be overcome to move it. The Peierls-Nabarro force plays an important role in the yield strengths of metals and alloys [114–116]. After the dislocation has moved by half a Burgers vector, the Peierls force pushes it forwards and moves it to the position of the next energy minimum. The Peierls force thus acts as a kind of frictional force and reduces the effective stress that can be used to drive the dislocation to overcome other obstacles.

In ordinary alloys, the Peierls-Nabarro force is a periodicallyvarying force in the crystal lattice due to the low concentration of solid solutions. However, in HEAs, this force is a non-periodic force due to the high concentration of solid solutions, as presented in Fig. 7. This trend also means that the movement of HEAs' dislocations needs to consume more energy, making them stronger than ordinary alloys [117]. It is also essential to investigate how other alloys overcome similar challenges. For example, He et al. [118] developed a strategy in medium manganese steels involving cold rolling, followed by low-temperature tempering. This process resulted in steels with metastable austenite grains embedded in a highly-dislocated martensite matrix, leading to both dislocation hardening and high ductility. The deformed and partitioned steel exhibited yield strengths of 2.21 and 2.05 GPa, respectively. Understanding the underlying principles in this strategy could help develop novel approaches for enhancing dislocation strengthening and ductility in HEAs. Another example that could inform the HEA research is the dislocation network structure observed in the 316L stainless steel produced using selective laser melting manufacturing, as reported by Liu et al. [3]. This method led to enhanced yield strength and ductility due to the high density of "flexible interfaces" that significantly tuned dislocation behaviors. By examining these examples and understanding the mechanisms at play, researchers can potentially develop innovative methods for optimizing the dislocation-strengthening mechanisms in HEAs.

2.6. Size effect

Size effects in materials can be broadly classified into two categories: grain-size and sample-size effects. Both of these size effects play a crucial role in determining the mechanical properties and overall performance of materials in various applications.

Grain boundaries are barriers to the dislocations' movement during the plastic deformation of the polycrystalline alloys. Generally, the strength of metals increases with decreasing grain size. Moreover, adjacent grains must be deformed to avoid material overlaps or gaps. Therefore, more slip systems must be activated

near grain boundaries to achieve compatible deformation of the grains, and they are more difficult to activate and require higher stresses.

Thus, grain-boundary strengthening contributes to the material's strength with an amount that is proportional to the inverse of the square root of the grain size. If we introduce a new proportionality constant, k, the amount of grain-boundary strengthening can be calculated by Eq. (8):

$$\Delta \sigma_{\rm Gs} = k/\sqrt{d} \tag{8}$$

where d is the grain size.

The advantage of grain-boundary strengthening is that the ductility of the material does not decrease with decreasing grain size and increasing strength, as long as the grain size remains in the coarse-grained region (>1 μ m) [119–121]. The tensile behavior of the HEAs with varied grain sizes has been widely studied [15,122–129]. Earlier work by Kumar et al. [126] presented the single-phase Al_{0.1}CoCrFeNi HEA, which was prepared by friction stir processing. He reduced the grain size of a single-phase Al_{0.1}CoCrFeNi HEA from millimetres to 14 \pm 10 μ m by friction stir processing. This process resulted in a substantial improvement of strength and ductility, compared with the as-cast condition, due to the enhanced grain refinement and a large fraction of high-angle grain boundaries. The high values of the Hall-Petch coefficients suggest that regulating grain size is an effective way to strengthen HEAs [122].

Severe plastic deformation is a more efficient technique to produce nano-scale and ultra-fine grains. It has been widely applied to refine the microstructure of various metallic materials. The ultrafine-grained $Al_{0.1}$ CoCrFeNi alloy was fabricated by cryo-rolling at the liquid nitrogen temperature and subsequent annealing [130]. It exhibits a high ultimate tensile strength above 1.0 GPa and a tensile strain larger than 20 %. The quantitative analysis of the grain-size dependence of strength suggests that a high lattice friction stress and a high grain-boundary strengthening are two major reasons for the strength-ductility balance. The trade-off between the strength and ductility results in an inverse relationship between the ultimate tensile strength and ductility.

The quantitative analysis of the grain-size dependence of strength suggests that a high lattice friction stress and a high grain-boundary strengthening are two major contributions to the excellent strength-ductility balance of the ultra-fine-grained HEAs. Table 1 lists the grain-size effect on the yield strength, ultimate tensile strength, and ductility of FeNiMnCoCr and Al_{0.3}CoCrFeNi alloys.

Sample-size effects, on the other hand, refer to the impact of the overall dimensions of a material sample on its mechanical properties. In micro- and nano-scale samples, such as micropillars or nanopillars, the sample size significantly affects properties like yield strength, flow stress, and strain hardening. This trend is primarily due to the reduced number of dislocations and other defects present in smaller samples, leading to a change in the governing deformation mechanisms. Sample-size effects often follow a power-law scaling, where properties, such as yield stress or flow stress, depend on the sample size with an inverse power-law exponent.

Three recent studies on HEAs reveal crucial insights into their mechanical properties and deformation mechanisms. Okamoto et al. [41] investigated the equiatomic CrMnFeCoNi HEA with an FCC structure and revealed a size-dependent critical resolved shear stress (CRSS), identified by an inverse power-law scaling exponent of -0.63. Zhang et al. [136] examined plastic-deformation mechanisms in single-crystalline HEAs with body-centered-cubic (BCC) phases, uncovering significant size effects on the yield/flow stress and remarkable strain hardening influenced by nanopillar orientation. Zhang et al. [137] also delved into the deformation behaviors and mechanisms of single-crystalline CoCrFeNi HEA mi-

Table 1Tensile properties of two typical HEAs in different grain sizes. Alongside shown is the information on the phase constitution, uniaxial yield strength, $\sigma_{0.2}$, ultimate tensile strength, σ_{us} , elongation to fracture, ε , average grain size, and testing temperature.

Alloy	d (μm)	$\sigma_{0.2}$ (MPa)	$\sigma_{ m uts}$ (MPa)	ε (%)	Temperature (°C)	Refs.
FeNiMnCoCr	0.65	800	888	27	298	[131]
	77	254	585	53	298	[132]
	4.4	350	650	60	293	[133]
	4.4	590	1,100	90	77	[133]
	30	300	676	41	298	[131]
	155	165	520	80	293	[133]
	155	350	900	105	77	[133]
	∞	510	1,580	60	296	[133]
	∞	240	980	58	77	[133]
Al _{0.3} CoCrFeNi	1.26	1,320	1,600	17.5	77	[134]
	1.26	1,136	1,207	11	298	[134]
	1.95	600	984	25	298	[134]
	2.13	588	968	26	298	[134]
	2.29	512	924	29	298	[134]
	2.30	516	930	30	298	[134]
	50	275	528	37	293	[135]
	∞	185	399	80	293	[135]

cro/nanopillars, identifying pronounced size effects on yield and flow stresses across different orientations. Nucleation and slip of full dislocations dominate the plastic deformation in <110> and <111>-oriented micro/nanopillars, while deformation twinning governs <100>-oriented micro/nanopillars. Large-scale atomistic simulations and a theoretical model help elucidate these deformation mechanisms, informing the design and fabrication of HEAs with high strength and remarkable plasticity.

Grain-size and sample-size effects are essential for tailoring the material strength and ductility properties. Investigating these size effects allows researchers to develop strategies for optimizing HEAs for a wide range of applications.

2.7. Heterogeneous structure

After applying torsion to cylindrical twinning-induced plasticity steel samples to generate a gradient nano-twinned structure along the radial direction, it was found that the yielding strength of the material can be doubled at no reduction in ductility [138]. It is shown that this evasion of strength-ductility trade-off is due to the formation of a gradient hierarchical nano-twinned structure during pre-torsion and subsequent tensile deformation [4,138–144]. Pan et al. [144] introduced gradient dislocations and grain boundaries in a single FCC phase Al_{0.1}CoCrFeNi alloy by cyclic torsion. This microstructure allows for high plasticity and enhances strength simultaneously. Moreover, the high-density stacking-faults-induced refined structure further improves the ductility and strength of this material.

An [145] summarized that structural hierarchy defeats alloy cracking. For example, eutectic high-entropy alloy (EHEA) develops a hierarchically organized herringbone microstructure that imparts multiscale crack buffering. This material exhibited exceptional damage tolerance over large tensile deformation, as well as ultrahigh uniform elongation. Hasan et al. [146] discovered that non-uniform elemental distributions in certain alloys can positively impact their mechanical performance. The enrichment of Mn and Ni at interdendritic boundaries occurred during the solidification process of the CrMnFeCoNi HEA, and this phenomenon was further intensified during dynamic deformation. The resulting alternation between soft and hard regions effectively impedes the propagation of adiabatic shear bands, thereby enhancing the material's toughness

Wu et al. [147] developed a methodology to design and fabricate ${\rm Al}_{0.1}{\rm CoCrFeNi}$ HEAs with a complex heterogeneous structure through cold working, followed by intermediate-temperature an-

nealing. The bulk HEAs possess a yield strength of 711 MPa, tensile strength of 928 MPa, and uniform elongation of 30.3 %. The enhancement of the strength-ductility trade-off is due to the microstructure comprised of a combination of the non-recrystallized and recrystallized grains arranged in complex heterogeneous structures with a characteristic dimension spanning from the submicron to coarse-sized scale. The initial heterogeneous structure of the HEA is composed of stretched grains, partially recrystallized grains, and recrystallized grains.

Fu et al. [148] also designed and implemented a heterogeneous grain structure to strengthen a single-phase Fe₂₉Ni₂₉Co₂₈Cu₇Ti₇ HEA. The heterostructured (HS) Fe₂₉Ni₂₉Co₂₈Cu₇Ti₇ HEA shows a dramatic enhancement (increasing from \sim 350 to \sim 614 MPa) in the tensile yield strength, as compared to its coarse-grain (CG) counterpart. The postannealed Fe₂₉Ni₂₉Co₂₈Cu₇Ti₇ HEA potentially exhibits a randomly distributed heterogeneous microstructure. Compared to its CG counterpart, the HS Fe₂₉Ni₂₉Co₂₈Cu₇Ti₇ HEA has a significant improvement in mechanical properties. This mechanism can be explained as follows: (1) Coarse and fine grains deform in an elastically similar manner to their homogeneous coarse-grained counterparts. (2) Deformation incompatibility of fine and coarse grains results in geometrically necessary dislocations (GND). Accordingly, the GNDs strengthen the soft coarse grains through forest-hardening and cross-slip mechanisms, leading to improved strength.

Shi et al. [149] used an AlCoCrFeNi_{2.1} alloy to engineer an ultrafine-grained duplex microstructure that deliberately inherits its composite lamellar nature by tailored thermo-mechanical processing to achieve property combinations. The samples exhibit hierarchically structural heterogeneities due to phase decomposition, and the improved mechanical response during deformation is attributed to both a two-hierarchical constraint effect and a self-generated microcrack-arresting mechanism. Shi et al. [148] also found self-buffering herringbone microstructure of eutectic HEA was extremely resistant to fracture. This trend is due to that the dynamic strain-hardened features prevent the crack from growing catastrophically and propagating rapidly. The material exhibits three times the plasticity of a non-buffering eutectic HEA without sacrificing strength.

The concept of designing heterogeneous structures involves identifying material parameters for specific properties. However, achieving precise control of the localized chemical and structural heterogeneities is challenging. Advanced manufacturing technologies, such as additive manufacturing, have the potential to realize

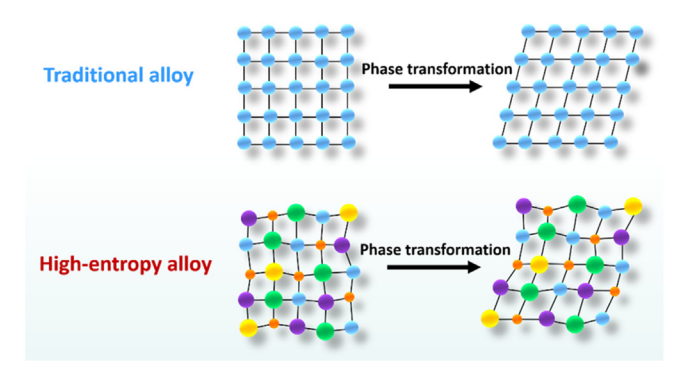


Fig. 8. Schematic diagram of the difference in martensitic transformation between traditional alloys and HEAs.

innovative heterogeneous structural alloy design concepts. This is achieved through the support of dedicated multiscale processing control.

2.8. Phase transformation

Phase transformations are important in the processing of metals and alloys, and they involve some alteration of the microstructure. In this summary, we mainly focus on martensitic transformation. This kind of phase transformation is diffusionless and instantaneous, wherein a metastable phase is produced.

HEAs studies presently favor single-phase, disordered solid-solution alloys [150,151]. Single-phase FCC HEAs usually display good ductility but relatively low strengths, while BCC HEAs are in the opposite [152]. In HEAs, the high proportion of different elements (e.g., Al, Fe, Mn, Ta, Nb, and W) may cause significant changes at the atom-lattice position. As such, they constitute a super solid solution that is capable of a much quicker transformation to other structures than traditional alloys if stress is applied (Fig. 8).

The metastability-engineering strategy has been widely used in high-manganese steels and titanium alloys. This approach can also be applied to the HEAs field [153–155], for instance, the Fe_{80-x}Mn_xCo₁₀Cr₁₀ and Ta_xHfZrTi HEA systems [54,55]. The mechanical behavior of the newly developed Fe₅₀Mn₃₀Co₁₀Cr₁₀ HEAs is superior to various single-phase HEAs. The underlying idea is to destabilize the high-temperature FCC phase via changing the Mn or Ta content, which promotes the TRIP effect. Consequently, both the strength and ductility were significantly increased due to the concurrent interface hardening from the dual-phase microstructure and transformation hardening from the metastability [156].

Raabe et al. [127] have tailored microstructures of the TRIP $Fe_{50}Mn_{30}Co_{10}Cr_{10}$ HEA to obtain higher values of the strength-ductility product index. The combination of the fine grain size and distribution of small volume fractions of HCP phases leads to the high work-hardening rate over an extended plastic strain range due to an enhanced TRIP effect.

In many instances, the preferred state for numerous important alloys is a metastable one, intermediate between the initial and equilibrium states. Sometimes, a microstructure far removed from the equilibrium one is desired. Therefore, it is crucial to investigate the influence of time-dependent phase transformations on highentropy alloys (HEAs). This information is often more valuable than knowing the final equilibrium state alone.

2.9. Composite structure

The observed mechanical properties trade-off in metamaterials is due to competition between the strengthening and toughening mechanisms in materials. Fabricating composite materials is

a vital approach to evade such a trade-off to optimize the properties of mechanical metamaterials. Until now, research on highentropy composite materials is rare. Zhang et al. [63] created an octet-truss composite nano-lattice made of two constituent materials, a polymer core, and an HEA coating that overcome the strength-recoverability trade-off. The light and ductile polymer core serves as a frame for allowing the whole structure to recover after large deformation, while the ultra-strong HEA coating improves the strength. The polymer-HEA composite nanolattices simultaneously achieve high strength and good recoverability, thereby overcoming the strength-recoverability trade-off. During compression to a strain of 50 %, the maximum strength of the composite nano-lattice reaches 11.6 MPa, leading to an energy absorption per unit volume of 4.0 MJ/m³, which is higher than that of most natural materials (such as bone, antler, and calcite) and micro/nano-lattices reported previously.

2.10. Preparation-method effect

The preparation method plays a critical role in determining the mechanical properties of HEAs, as it influences the microstructure, phase composition, and distribution of elements. Traditional techniques, such as casting [157-159] and powder metallurgy [160,161], have been widely used to prepare HEAs, but they often struggle to overcome the strength-ductility trade-off due to the formation of coarse grains, inhomogeneous elemental distribution, and presence of brittle intermetallic phases. Additive manufacturing (AM) has emerged as an advanced technique for producing HEAs with the potential to break the strength-ductility tradeoff [162-164]. The AM techniques, such as selective laser melting (SLM) [165-167] and electron beam melting (EBM) [168,169], enable the fabrication of complex geometries and the tailoring of microstructures through the precise control of processing parameters. Rapid solidification and cooling rates associated with AM lead to the formation of refined grain structures, uniform elemental distribution, and metastable phases, all of which can contribute to the improved strength and ductility in HEAs [77]. Moreover, the flexibility offered by AM facilitates the design and optimization of novel HEA compositions and microstructures, paving the way for the development of high-performance materials with enhanced mechanical properties for a wide range of applications.

The ductility of AM-produced HEAs can vary, depending on the specific alloy system and processing parameters [170,171]. In some cases, the rapid cooling rates associated with AM processes can lead to the formation of highly disordered microstructures with a reduced number of brittle intermetallic phases, which can improve the ductility of the resulting alloy [172]. However, in other cases, the high residual stresses and porosity often observed in AM-produced components can have a negative impact on ductility [173]. Careful control of the processing parameters and post-processing heat treatments can help mitigate these issues and optimize the ductility of AM-produced HEAs.

When comparing the strength and ductility of AM-produced HEAs to those manufactured using traditional methods, several factors should be considered. The microstructures of AM-produced HEAs are typically more refined and homogeneous, compared to those of traditionally fabricated counterparts. This feature can lead to an improvement in both strength and ductility for the AM-produced alloys. However, the presence of porosity and residual stresses in AM components can counteract these benefits and negatively impact their mechanical properties.

The processing parameters used during the AM process can significantly influence the mechanical properties of the resulting HEA components. For example, adjusting the laser power, scan speed, and layer thickness in SLM can help optimize the balance between strength and ductility by controlling the solidification behavior

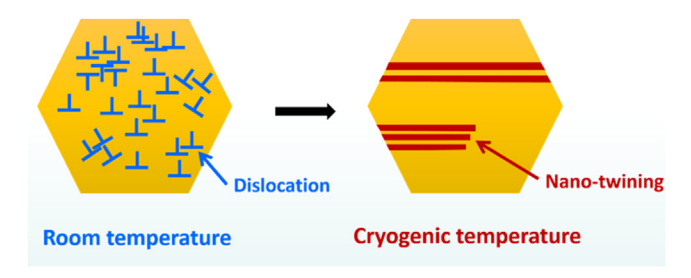


Fig. 9. Schematic diagram of the deformation mechanisms at room and cryogenic temperatures.

and resulting microstructure [174,175]. Post-processing techniques, such as heat treatments and hot-isostatic pressing, can be employed to further refine the microstructures and alleviate residual stresses in AM-produced HEAs [176–178]. These treatments can help enhance both the strength and ductility of the components, making them more comparable or even superior to their traditionally fabricated counterparts.

In conclusion, AM holds great potential for producing highperformance HEA components with improved strength and ductility, compared to traditional manufacturing methods. However, careful control of the processing parameters and post-processing treatments is crucial to fully harness the advantages of AM for HEA production.

2.11. Temperature effect

In addition to slip, plastic deformation in some metallic materials can also occur through the formation of mechanical twins [179-182]. Mechanical twinning occurs in metals at low temperatures, shock loading, and conditions under which the slip process is restricted. The amount of the bulk plastic deformation from twinning is normally small, relative to that resulting from slip. However, the real importance of twinning lies with the accompanying crystallographic reorientations. Mechanical twinning may place new slip systems in orientations that are favorable, relative to the stress axis such that the slip process can now take place [183]. For HEAs, the deformation mechanism at low temperatures is transformed from the dislocation slip to mechanical nano-twinning [57–59,84,184], as presented in Fig. 9. Extensive dislocation-twin boundaries interactions are propitious to the enhancement of the strain-hardening and then ductility [17]. This feature makes the mechanical properties of HEAs exhibit excellent plasticity and strength at cryogenic temperatures. The temperature dependence of the yield strength can be expressed as the sum of thermal (σ_{th}) and athermal (σ_{ath}) components [60,185]:

$$\sigma_{y} = \sigma_{th} + \sigma_{ath} \tag{9}$$

where $\sigma_{\rm th}$ is the thermal contribution, which corresponds to the thermal activation of dislocation motion, and $\sigma_{\rm ath}$ is an athermal contribution, which is independent of the temperature.

In addition to tailoring the microstructure, temperature could also change the deformation to encourage strain-hardening mechanisms during deformation [179,180,186–188]. A prominent example is an equiatomic HEA with the composition of FeMnNiCoCr, which showed excellent strength, ductility, and fracture toughness at cryogenic and room temperatures [56,60,62,179,189]. Mechanical properties of a typical FeMnNiCoCr HEA improve at cryogenic temperatures [56]. This trend is due to a transition from the planar-slip dislocation activity at room temperature to deformation by mechanical nano-twinning with decreasing temperature, which results in continuous steady strain hardening.

The quaternary CoCrFeNi HEA [190] also shows high strength and ductility in the cryogenic environment. The strength and duc-

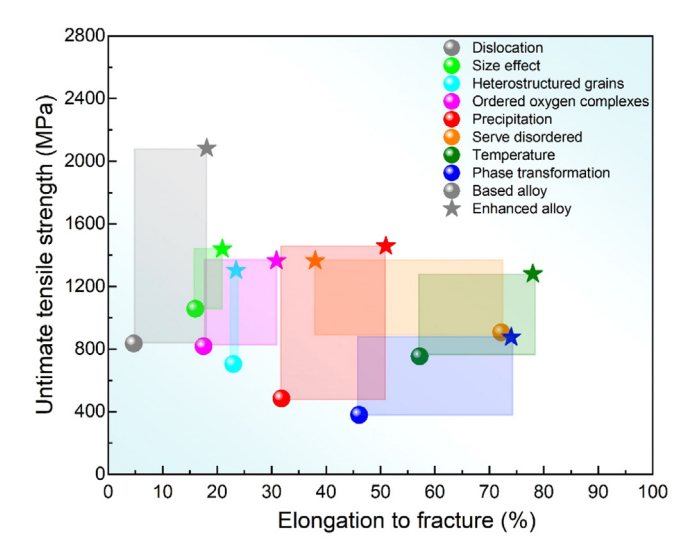


Fig. 10. A summary of reported routes for overcoming strength-ductility trade-off in HEAs, for instance, dislocation [118], grain size [191], heterostructured grains [148], ordered oxygen complexes [53], precipitation [52], severely disordered lattice [109], temperature [56], and phase transformation [54].

tility can be ascribed to the low stacking fault energy at extremely low temperatures. The low stacking fault energy facilitates the activation of deformation twinning and phase transformation at the liquid helium temperature, which produces a high strain-hardening rate to sustain the stable plastic flow.

In conclusion, we sum up the typical examples to break the strength-ductility trade-off in Fig. 10. Different methods affect the strength and plasticity of the alloy to varying degrees. However, these seemingly distinct tactics share a unifying design principle in tailoring the microstructure, especially defects, to enhance strain hardening and consequently, uniform tensile ductility at high stresses. Furthermore, there are still multiple facets that can affect the final properties of alloys deserved for detailed understanding.

Fig. 11 shows a comparison of yield and tensile properties of HEAs with various traditional alloys. It is obvious that HEAs are separated from the common trend for conventional metallic materials, suggesting a favorable strength-ductility combination. This trend reveals that although overcoming the strength-ductility trade-off has been challenging in the past, it is now promising to achieve great tensile strength and ductility simultaneously in HEAs due to the original design concept and mechanisms.

3. Future work

High-entropy alloys (HEAs) have gained significant interest due to their potential to surpass the property limits of current materials. To advance our understanding, design, and applications of HEAs, future research should focus on key areas.

For instance, even with recent advancements in computational techniques, accurately predicting the properties of HEAs remains challenging due to their complex compositions. Future research should prioritize developing and refining computational models, utilizing machine learning and artificial intelligence to predict HEA properties, phase stability, and microstructures. Moreover, attention should be given to the development of rapid synthesis and characterization methods and the investigation of minor alloying elements and entropy effects. Furthermore, emphasizing environmentally friendly HEAs and interdisciplinary collaboration will be essential for promoting sustainable technology development and facilitating accelerated industry adoption.

The exploration of advanced processing techniques, such as additive manufacturing and novel heat treatments, is crucial for op-

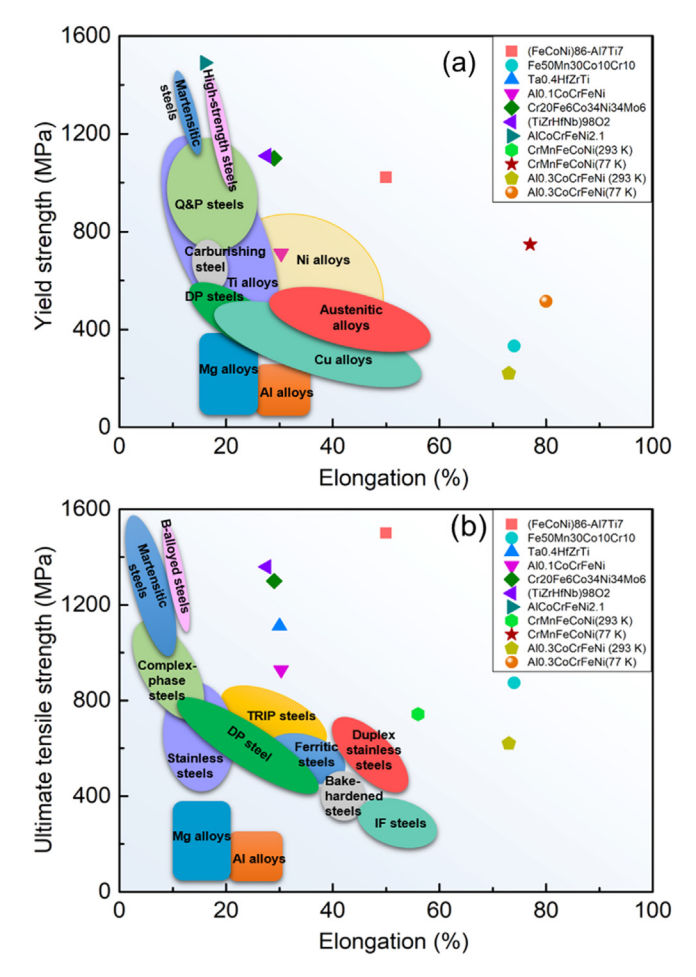


Fig. 11. (a) Yield and (b) ultimate tensile properties of traditional alloys and HEAs overcoming the strength-ductility trade-off [52-56,62,143,147,191].

timizing microstructures and properties of HEAs, ultimately resulting in high-performance materials with superior mechanical and functional attributes. Furthermore, in-situ and operando characterization techniques will offer valuable insights into the evolution of microstructures, phase transformations, and mechanical behavior of HEAs under various conditions, which will benefit their realworld applications and performance optimization.

Tackling challenges related to scale-up and industrial adoption is vital for the long-term success of HEAs. This involves developing cost-effective, scalable production methods, establishing robust quality control systems, and ensuring the long-term performance and reliability of HEA components across a range of applications. Addressing these challenges will enable more widespread integration of HEAs into various industries.

By focusing on these future work areas, we aim to not only advance the understanding, design, and application of high-entropy alloys but also contribute to the development of next-generation materials that outperform current ones. This advancement will ultimately lead to innovative technologies and sustainable solutions across diverse industries, enhancing our quality of life and promoting a more sustainable future.

4. Summary

The strength-ductility trade-off has been a long-standing dilemma in materials science. This feature has limited the potential of many structural materials, alloys in particular. However, a few methods have shown the capability of improving strength while

retaining the ductility of materials. We summarized the mechanical properties and deformation behavior of HEAs and reviewed the proposed strengthening-toughening strategies and corresponding deformation mechanisms. In the approaches to achieve enhanced strength or ductility for the HEAs, the common theme is tailoring microstructures by manipulating the microstructures, for instance, twins, dislocations, second phases, precipitates, grain boundaries, short range order, etc. The alternative is to take advantage of the dependence of the flow mechanism on deformation conditions. Thus, appropriate deformation conditions can be employed to make use of the elevated strain-rate hardening capability of some materials. The result is a simultaneous enhancement of strength and ductility, rather than one of them alone.

These research directions offer numerous new opportunities. As evident from previous discussions, many poorly explained observations and unexplored territories remain. For almost every approach, there are arguments that need to be substantiated and better analyzed. Future research should focus on addressing these knowledge gaps, refining our understanding of the underlying mechanisms, and further exploring the potential of HEAs to overcome the strength-ductility trade-off, ultimately paving the way for the development of advanced materials with superior mechanical properties for a wide range of applications.

Author contributions

The original idea was conceived by Dongyue Li, Yong Zhang, and Wenrui Wang. All authors discussed and commented on the manuscript.

Declaration of competing interest

The authors declare that they have no known competing financial interests or personal relationships that could have appeared to influence the work reported in this paper.

Acknowledgements

The authors would like to gratefully acknowledge the financial support from the National Natural Science Foundation of China (Nos. 52101189 and 52273280) and the National Key R&D Program of China (No. 2020YFA0405700). The present work was also supported by the Chinese Postdoctoral Science Foundation (No. 2020M680343) and the Fundamental Research Funds for the Central Universities (No. FRF-TP-20-050A1). PKL thanks the support from the National Science Foundation (Nos. DMR-1611180, 1809640, and 2226508) and the Army Research Office (Nos. W911NF-13-1-0438 and W911NF-19-2-0049).

References

- [1] G. Da Silveira, N. Slack, Int. J. Oper. Prod. Manage. 21 (2001) 949-964.
- [2] A.M. Madni, A. Ross, Using Tradeoff Analyses to Identify Value and Risk, Wiley, New York, 2016.
- [3] L. Liu, Q. Ding, Y. Zhong, J. Zou, J. Wu, Y.L. Chiu, J. Li, Z. Zhang, Q. Yu, Z. Shen, Mater. Today 21 (2018) 354-361.
- E. Ma, T. Zhu, Mater. Today 20 (2017) 323-331.
- [5] U.G. Wegst, H. Bai, E. Saiz, A.P. Tomsia, R.O. Ritchie, Nat. Mater. 14 (2015) 23.
- Y. Zhao, T. Topping, Y. Li, E.J. Lavernia, Adv. Eng. Mater. 13 (2011) 865–871. Y. Zhao, E. Lavernia, Nanostruct. Met. Alloy. (2011) 375–429.
- [8] S.H. Whang, in: Nanostructured Metals and Alloys: Processing, Microstructure, Mechanical Properties and Applications, Elsevier, 2011, pp. 787–803.
- [9] J.W. Yeh, S.K. Chen, S.J. Lin, J.Y. Gan, T.S. Chin, T.T. Shun, C.H. Tsau, S.Y. Chang, Adv. Eng. Mater. 6 (2004) 299-303.
- [10] X. Fu, C.A. Schuh, E.A. Olivetti, Scr. Mater. 138 (2017) 145-150.
- [11] B. Cantor, I.T.H. Chang, P. Knight, A.J.B. Vincent, Mater. Sci. Eng. A 375-377 $(2004)\ 213-218$
- Y. Zhang, M. Zhang, D. Li, T. Zuo, K. Zhou, M.C. Gao, B. Sun, T. Shen, Metals 9 (2019) 1-14
- [13] T. Yang, W. Guo, J.D. Poplawsky, D. Li, L. Wang, Y. Li, W. Hu, M.L. Crespillo, Z. Yan, Y. Zhang, Acta Mater. 188 (2020) 1-15.

- [14] D. Wei, W. Gong, T. Tsuru, I. Lobzenko, X. Li, S. Harjo, T. Kawasaki, H.S. Do, J.W. Bae, C. Wagner, Int. J. Plast. 159 (2022) 103443.
- [15] Y. Wang, M. Chen, F. Zhou, E. Ma, Nature 419 (2002) 912-915.
- [16] S.H. Kim, H. Kim, N.J. Kim, Nature 518 (2015) 77-79.
- [17] L. Lu, X. Chen, X. Huang, K. Lu, Science 323 (2009) 607-610.
- [18] S. Zhao, R. Zhang, Q. Yu, J. Ell, R.O. Ritchie, A.M. Minor, Science 373 (2021) 1363-1368.
- [19] Y.H. Zhao, I.F. Bingert, X.Z. Liao, B.Z. Cui, K. Han, A.V. Sergueeva, A.K. Mukherjee, R.Z. Valiev, T.G. Langdon, Y.T. Zhu, Adv. Mater. 18 (2006) 2949-2953
- [20] Z. Ma, W. Zhang, H. Zhao, F. Lu, Z. Zhang, L. Zhou, L. Ren, J. Alloy. Compd. 817 (2020) 152709.
- [21] W. Zhang, Z. Ma, H. Zhao, L. Ren, Mater. Sci. Eng. A 800 (2021) 140264.
- [22] W. Zhang, Z. Ma, H. Zhao, L. Ren, Mater. Sci. Eng. A 847 (2022) 143343.
- [23] W. Zhang, Z. Ma, C. Li, C. Guo, D. Liu, H. Zhao, L. Ren, J. Mater. Sci. Technol. 114 (2022) 102-110
- [24] Y. Guo, L. Liu, Y. Zhang, J. Qi, B. Wang, Z. Zhao, J. Shang, J. Xiang, J. Mater. Res. 33 (2018) 3258-3265.
- [25] J. He, H. Wang, H. Huang, X. Xu, M. Chen, Y. Wu, X. Liu, T. Nieh, K. An, Z. Lu, Acta Mater. 102 (2016) 187-196.
- [26] Y.J. Liang, L. Wang, Y. Wen, B. Cheng, Q. Wu, T. Cao, Q. Xiao, Y. Xue, G. Sha, Y. Wang, Nat. Commun. 9 (2018) 4063.
- S. Cheng, Y. Zhao, Y. Zhu, E. Ma, Acta Mater. 55 (2007) 5822-5832.
- [28] Y.H. Zhao, Trans. Nonferrous Met. Soc. China 31 (2021) 1205-1216.
- [29] Y.-H. Zhao, X.Z. Liao, S. Cheng, E. Ma, Y.T. Zhu, Adv. Mater. 18 (2006) 2280-2283.
- [30] E.P. George, D. Raabe, R.O. Ritchie, Nat. Rev. Mater. 4 (2019) 515-534.
- [31] J.W. Yeh, Ann. Chim. Sci. Matér. 31 (2006) 633-648.
- [32] Y. Zhang, T.T. Zuo, Z. Tang, M.C. Gao, K.A. Dahmen, P.K. Liaw, Z.P. Lu, Prog. Mater. Sci. 61 (2014) 1-93.
- [33] D.B. Miracle, O.N. Senkov, Acta Mater. 122 (2017) 448-511.
- Z. Li, S. Zhao, R.O. Ritchie, M.A. Meyers, Prog. Mater. Sci. 7 (2018) 3018.
- [35] B.S. Murty, J.W. Yeh, S. Ranganathan, P. Bhattacharjee, in: High-Entropy Alloys, Elsevier, 2019, pp. 1-9.
- G. Sheng, C.T. Liu, Prog. Nat. Sci. 21 (2011) 433-446.
- [37] E.P. George, W. Curtin, C.C. Tasan, Acta Mater. 188 (2020) 435-474.
- [38] M.H. Tsai, J.W. Yeh, Mater. Res. Lett. 2 (2014) 107-123.
- Z. Lu, H. Wang, M. Chen, I. Baker, J. Yeh, C.T. Liu, T. Nieh, Intermetallics 66 (2015) 67-76.
- [40] Y. Lu, X. Gao, L. Jiang, Z. Chen, T. Wang, J. Jie, H. Kang, Y. Zhang, S. Guo, H. Ruan, Acta Mater. 124 (2017) 143-150.
- N.L. Okamoto, S. Fujimoto, Y. Kambara, M. Kawamura, Z.M. Chen, H. Mat-
- sunoshita, K. Tanaka, H. Inui, E.P. George, Sci. Rep. 6 (2016) 35863. [42] H. Kong, J. Tao, C. Liu, S. Ying, K. Zhao, Mater. Rep. 34 (2020) 14134-14139.
- [43] D. Li, M.C. Gao, J.A. Hawk, Y. Zhang, J. Alloy. Compd. 778 (2019) 23-29.
- [44] R.R. Eleti, T. Bhattacharjee, A. Shibata, N. Tsuji, Acta Mater. 171 (2019)
- 132-145. [45] A. Takeuchi, K. Amiya, T. Wada, K. Yubuta, W. Zhang, JOM 66 (2014)
- 1984-1992. Y. Zhao, J. Qiao, S. Ma, M. Gao, H. Yang, M. Chen, Y. Zhang, Mater. Des. 96 (2016) 10-15.
- [47] R. Soler, A. Evirgen, M. Yao, C. Kirchlechner, F. Stein, M. Feuerbacher, D. Raabe, G. Dehm, Acta Mater. 156 (2018) 86-96.
- [48] M.C. Gao, B. Zhang, S. Guo, J. Qiao, J. Hawk, Metall. Mater. Trans. A 47 (2016) 3322-3332.
- [49] M. Feuerbacher, M. Heidelmann, C. Thomas, Mater. Res. Lett. 3 (2015) 1-6.
- [50] S. Cheng, H. Choo, Y. Zhao, X.L. Wang, Y. Zhu, Y. Wang, J. Almer, P. Liaw, J. Jin, Y. Lee, J Mater. Res. 23 (2008) 1578-1586.
- [51] O.N. Senkov, D.B. Miracle, K.J. Chaput, J.P. Couzinie, J Mater. Res. 33 (2018)
- [52] T. Yang, Y. Zhao, Y. Tong, Z. Jiao, J. Wei, J. Cai, X. Han, D. Chen, A. Hu, J. Kai, Science 362 (2018) 933–937.
- Z. Lei, X. Liu, Y. Wu, H. Wang, S. Jiang, S. Wang, X. Hui, Y. Wu, B. Gault, P. Kontis, Nature 563 (2018) 546.
- [54] Z. Li, K.G. Pradeep, Y. Deng, D. Raabe, C.C. Tasan, Nature 534 (2016) 227-230. [55] H. Huang, Y. Wu, J. He, H. Wang, X. Liu, K. An, W. Wu, Z. Lu, Adv. Mater.
- (2017) 29. [56] B. Gludovatz, A. Hohenwarter, D. Catoor, E.H. Chang, E.P. George, R.O. Ritchie,
- Science 345 (2014) 1153-1158. [57] Y.H. Jo, S. Jung, W.M. Choi, S.S. Sohn, H.S. Kim, B.J. Lee, N.J. Kim, S. Lee, Nat.
- Commun. 8 (2017) 15719.
- [58] B. Gludovatz, A. Hohenwarter, K.V. Thurston, H. Bei, Z. Wu, E.P. George, R.O. Ritchie, Nat. Commun. 7 (2016) 10602.
- [59] N. Stepanov, M. Tikhonovsky, N. Yurchenko, D. Zyabkin, M. Klimova, S. Zherebtsov, A. Efimov, G. Salishchev, Intermetallics 59 (2015) 8-17.
- [60] S.J. Sun, Y.Z. Tian, H.R. Lin, H.J. Yang, X.G. Dong, Y.H. Wang, Z.F. Zhang, Mater. Sci. Eng. A 740 (2019) 336-341. [61] W. Huo, F. Fang, H. Zhou, Z. Xie, J. Shang, J. Jiang, Scr. Mater. 141 (2017)
- 125-128.
- [62] D. Li, Y. Zhang, Intermetallics 70 (2016) 24-28.
- [63] X. Zhang, J. Yao, B. Liu, J. Yan, L. Lu, Y. Li, H. Gao, X. Li, Nano Lett. 18 (2018) 4247-4256.
- Y. Yao, Z. Huang, P. Xie, S.D. Lacey, R.J. Jacob, H. Xie, F. Chen, A. Nie, T. Pu, M. Rehwoldt, Science 359 (2018) 1489-1494.
- [65] Y. Tong, D. Chen, B. Han, J. Wang, R. Feng, T. Yang, C. Zhao, Y. Zhao, W. Guo, Y. Shimizu, Acta Mater. 165 (2019) 228-240.

- [66] H. Diao, D. Ma, R. Feng, T. Liu, C. Pu, C. Zhang, W. Guo, J.D. Poplawsky, Y. Gao, P.K. Liaw, Mater. Sci. Eng. A 742 (2019) 636-647.
- [67] T. Yang, Y. Zhao, J. Luan, B. Han, J. Wei, J. Kai, C. Liu, Scr. Mater. 164 (2019) 30-35.
- [68] Y. Zhao, H. Chen, Z. Lu, T. Nieh, Acta Mater. 147 (2018) 184-194.
- [69] E. Pickering, R. Muñoz-Moreno, H.J. Stone, N.G. Jones, Scr. Mater. 113 (2016) 106-109.
- [70] G. Laplanche, S. Berglund, C. Reinhart, A. Kostka, F. Fox, E. George, Acta Mater. 161 (2018) 338-351.
- [71] Z. Zhang, D. Chen, Scr. Mater. 54 (2006) 1321-1326.
- [72] C. Booth-Morrison, D.C. Dunand, D.N. Seidman, Acta Mater. 59 (2011) 7029-7042.
- [73] P. Pandey, S. Kashyap, D. Palanisamy, A. Sharma, K. Chattopadhyay, Acta Mater. 177 (2019) 82-95.
- [74] B. Gwalani, V. Soni, M. Lee, S. Mantri, Y. Ren, R. Banerjee, Mater. Des. 121 (2017) 254-260.
- [75] L. Liu, Y. Zhang, J. Han, X. Wang, W. Jiang, C.T. Liu, Z. Zhang, P.K. Liaw, Adv. Sci. 8 (2021) 2100870.
- [76] T. Yang, Y. Zhao, L. Fan, J. Wei, J. Luan, W. Liu, C. Wang, Z. Jiao, J. Kai, C. Liu, Acta Mater. 189 (2020) 47-59.
- [77] J. Shen, P. Agrawal, T.A. Rodrigues, J. Lopes, N. Schell, J. He, Z. Zeng, R.S. Mishra, J. Oliveira, Mater. Sci. Eng. A 867 (2023) 144722.
- [78] L. Chen, R. Wei, K. Tang, J. Zhang, F. Jiang, L. He, J. Sun, Mater. Sci. Eng. A 716 (2018) 150-156.
- [79] J.B. Seol, J.W. Bae, Z. Li, J.C. Han, J.G. Kim, D. Raabe, H.S. Kim, Acta Mater. 151 (2018) 366-376.
- [80] X. An, S. Wu, Z. Wang, Z. Zhang, Prog. Mater. Sci. 101 (2019) 1-45.
- X. An, Q. Lin, S. Wu, Z. Zhang, R. Figueiredo, N. Gao, T. Langdon, Scr. Mater. 64 (2011) 954-957.
- [82] Y. Chen, D. Chen, X. An, Y. Zhang, Z. Zhou, S. Lu, P. Munroe, S. Zhang, X. Liao, T. Zhu, Acta Mater. 215 (2021) 117112.
- [83] H. Wang, D. Chen, X. An, Y. Zhang, S. Sun, Y. Tian, Z. Zhang, A. Wang, J. Liu, M. Song, Sci. Adv. 7 (2021) 3105.
- [84] Q. Lin, J. Liu, X. An, H. Wang, Y. Zhang, X. Liao, Mater. Res. Lett. 6 (2018) 236-243.
- [85] S. Lu, X. Sun, Y. Tian, X. An, W. Li, Y. Chen, H. Zhang, L. Vitos, PNAS Nexus 2 (2023) 282.
- [86] X. Sun, S. Lu, R. Xie, X. An, W. Li, T. Zhang, C. Liang, X. Ding, Y. Wang, H. Zhang, Mater. Des. 199 (2021) 109396.
- [87] S. Ma, J. Zhang, B. Xu, Y. Xiong, W. Shao, S. Zhao, J. Alloy. Compd. 911 (2022) 165144.
- [88] Y. Wu, F. Zhang, X. Yuan, H. Huang, X. Wen, Y. Wang, M. Zhang, H. Wu, X. Liu, H. Wang, J. Mater. Sci. Technol. 62 (2021) 214-220.
- [89] R. Zhang, S. Zhao, J. Ding, Y. Chong, T. Jia, C. Ophus, M. Asta, R.O. Ritchie, A.M. Minor, Nature 581 (2020) 283-287.
- [90] T.J. Ziehl, D. Morris, P. Zhang, Iscience 26 (2023) 1-14.
- [91] J.B. Seol, J.W. Bae, J.G. Kim, H. Sung, Z. Li, H.H. Lee, S.H. Shim, J.H. Jang, W.-S. Ko, S.I. Hong, Acta Mater. 194 (2020) 366-377.
- [92] Y. Miyajima, T. Nagata, K. Takeda, S. Yoshida, S. Yasuno, C. Watanabe, I. Kazuhiro, H. Adachi, N. Tsuji, Sci. Rep. 12 (2022) 16776.
- [93] S. Mishra, S. Maiti, B.S. Dwadasi, B. Rai, Sci. Rep. 9 (2019) 1-11.
- [94] R. Niu, X. An, L. Li, Z. Zhang, Y.W. Mai, X. Liao, Acta Mater. 223 (2022) 117460.
- [95] S. Chen, Z.H. Aitken, S. Pattamatta, Z. Wu, Z.G. Yu, D.J. Srolovitz, P.K. Liaw, Y.-W. Zhang, Nat. Commun. 12 (2021) 4953.
- [96] P. Singh, A.V. Smirnov, A. Alam, D.D. Johnson, Acta Mater. 189 (2020) 248-254.
- [97] H.W. Hsiao, R. Feng, H. Ni, K. An, J.D. Poplawsky, P.K. Liaw, J.M. Zuo, Nat. Commun. 13 (2022) 6651.
- [98] B. Yin, S. Yoshida, N. Tsuji, W. Curtin, Nat. Commun. 11 (2020) 2507.
- [99] H. Song, F. Tian, Q.M. Hu, L. Vitos, Y. Wang, J. Shen, N. Chen, Phys. Rev. Mater. 1 (2017) 023404.
- [100] C. Lee, G. Song, M.C. Gao, R. Feng, P. Chen, J. Brechtl, Y. Chen, K. An, W. Guo, J.D. Poplawsky, Acta Mater. 160 (2018) 158-172.
- [101] Y. Tong, K. Jin, H. Bei, J. Ko, D.C. Pagan, Y. Zhang, F. Zhang, Mater. Des. 155 (2018) 1-7
- [102] Z. Wang, Q. Fang, J. Li, B. Liu, Y. Liu, J. Mater. Sci. Technol. 34 (2018) 349-354.
- [103] L. Owen, E. Pickering, H. Playford, H.J. Stone, M. Tucker, N.G. Jones, Acta Mater. 122 (2017) 11-18.
- [104] C.R. LaRosa, M. Shih, C. Varvenne, M. Ghazisaeidi, Mater. Charact. 151 (2019) 310-317
- [105] F.G. Coury, M. Kaufman, A.J. Clarke, Acta Mater. 175 (2019) 66–81.[106] S. Gorsse, D.B. Miracle, O.N. Senkov, Acta Mater. 135 (2017) 177–187.
- [107] T. Borkar, B. Gwalani, D. Choudhuri, C. Mikler, C. Yannetta, X. Chen, R.V. Ramanujan, M. Styles, M. Gibson, R. Banerjee, Acta Mater. 116 (2016) 63-76.
- [108] C.G. Schön, T. Duong, Y. Wang, R. Arróyave, Acta Mater. 148 (2018) 263-279.
- [109] S.S. Sohn, A. Kwiatkowski da Silva, Y. Ikeda, F. Körmann, W. Lu, W.S. Choi, B. Gault, D. Ponge, J. Neugebauer, D. Raabe, Adv. Mater. 31 (2019) 1807142.
- [110] Y. Zhao, T. Yang, Y. Tong, J. Wang, J. Luan, Z. Jiao, D. Chen, Y. Yang, A. Hu, C. Liu, Acta Mater. 138 (2017) 72-82
- [111] X. Li, Y. Wei, L. Lu, K. Lu, H. Gao, Nature 464 (2010) 877-880.
- [112] X. Xu, P. Liu, Z. Tang, A. Hirata, S. Song, T. Nieh, P. Liaw, C. Liu, M. Chen, Acta Mater. 144 (2018) 107-115.
- [113] Y. Deng, C.C. Tasan, K.G. Pradeep, H. Springer, A. Kostka, D. Raabe, Acta Mater. 94 (2015) 124-133.
- [114] L. Zhang, Y. Xiang, J. Han, D.J. Srolovitz, Acta Mater. 166 (2019) 424-434.

- [115] Z. Pei, Mater. Sci. Eng. A 737 (2018) 132-150.
- [116] X. Liu, Z. Pei, M. Eisenbach, Mater. Des. 180 (2019) 107955.
- [117] B. Gwalani, S. Gorsse, D. Choudhuri, Y. Zheng, R.S. Mishra, R. Banerjee, Scr. Mater, 162 (2019) 18–23.
- [118] B. He, B. Hu, H. Yen, G. Cheng, Z. Wang, H. Luo, M. Huang, Science 357 (2017) 1029–1032.
- [119] N. Hansen, Scr. Mater. 51 (2004) 801-806.
- [120] L. Zhang, Y. Shibuta, Mater. Lett. 274 (2020) 128024.
- [121] S. Chen, Z.H. Aitken, Z. Wu, Z. Yu, R. Banerjee, Y.-W. Zhang, Mater. Sci. Eng. A 773 (2020) 138873.
- [122] W.H. Liu, Y. Wu, J.Y. He, T.G. Nieh, Z.P. Lu, Scr. Mater. 68 (2013) 526-529.
- [123] B. Gwalani, V. Soni, M. Lee, S.A. Mantri, Y. Ren, R. Banerjee, Mater. Des. 121 (2017) 254–260.
- [124] F. Yin, G.J. Cheng, R. Xu, K. Zhao, Q. Li, J. Jian, S. Hu, S. Sun, L. An, Q. Han, Scr. Mater. 155 (2018) 26–31.
- [125] S. Gangireddy, B. Gwalani, R.S. Mishra, Mater. Sci. Eng. A 736 (2018) 344-348.
- [126] N. Kumar, M. Komarasamy, P. Nelaturu, Z. Tang, P. Liaw, R. Mishra, JOM 67 (2015) 1007–1013.
- [127] D. Raabe, K.C. Cho, K. Liu, M. Frank, R.E. Brennan, R.S. Mishra, S.S. Nene, Z. Li, Sci. Rep. 7 (2017) 16167.
- [128] B. Schuh, B. Völker, J. Todt, N. Schell, L. Perrière, J. Li, J. Couzinié, A. Hohenwarter, Acta Mater. 142 (2018) 201–212.
- [129] Z. Li, C.C. Tasan, K.G. Pradeep, D. Raabe, Acta Mater. 131 (2017) 323-335.
- [130] X. Xu, P. Liu, A. Hirata, S. Song, T. Nieh, M. Chen, Materialia 4 (2018) 395–405.
- [131] Y.Z. Tian, S.J. Sun, H.R. Lin, Z.F. Zhang, J. Mater. Sci. Technol. 35 (2019) 334–340.
- [132] K. Suzuki, M. Koyama, H. Noguchi, Proc. Struct. Integr. 13 (2018) 1065-1070.
- [133] I. Kireeva, Y. Chumlyakov, Z. Pobedennaya, D. Kuksgauzen, I. Karaman, H. Sehitoglu, in: Proceeding of the American Institute of Physics Conference Series, AIP Publishing LLC, November 10, 2016.
- [134] D. Li, C. Li, T. Feng, Y. Zhang, G. Sha, J.J. Lewandowski, P.K. Liaw, Y. Zhang, Acta Mater. 123 (2017) 285–294.
- [135] S.G. Ma, S.F. Zhang, J.W. Qiao, Z.H. Wang, M.C. Gao, Z.M. Jiao, H.J. Yang, Y. Zhang, Intermetallics 54 (2014) 104–109.
- [136] Q. Zhang, R. Huang, X. Zhang, T. Cao, Y. Xue, X. Li, Nano Lett. 21 (2021) 3671–3679.
- [137] Q. Zhang, R. Huang, J. Jiang, T. Cao, Y. Zeng, J. Li, Y. Xue, X. Li, J. Mech. Phys. Solids 162 (2022) 104853.
- [138] Y. Wei, Y. Li, L. Zhu, Y. Liu, X. Lei, G. Wang, Y. Wu, Z. Mi, J. Liu, H. Wang, Nat. Commun. 5 (2014) 3580.
- [139] S. Shukla, T. Wang, S. Cotton, R.S. Mishra, Scr. Mater. 156 (2018) 105-109.
- [140] Y. Zhou, X. Jin, L. Zhang, X. Du, B. Li, Mater. Sci. Eng. A 716 (2018) 235–239.
- [141] Z. Fu, L. Jiang, J.L. Wardini, B.E. MacDonald, H. Wen, W. Xiong, D. Zhang, Y. Zhou, T.J. Rupert, W. Chen, Sci. Adv. 4 (2018) 8712.
- [142] M. Hasan, Y. Liu, X. An, J. Gu, M. Song, Y. Cao, Y. Li, Y. Zhu, X. Liao, Int. J. Plast. 123 (2019) 178–195.
- [143] K. Ming, X. Bi, J. Wang, Int. J. Plast. 113 (2019) 255-268.
- [144] Q. Pan, L. Zhang, R. Feng, Q. Lu, K. An, A.C. Chuang, J.D. Poplawsky, P.K. Liaw, L. Lu, Science 374 (2021) 984–989.
- [145] X. An, Science 373 (2021) 857–858.
- [146] M. Hasan, J. Gu, S. Jiang, H. Wang, M. Cabral, S. Ni, X. An, M. Song, L. Shen, X. Liao, Scr. Mater. 190 (2021) 80–85.
- [147] S. Wu, G. Wang, Q. Wang, Y. Jia, J. Yi, Q. Zhai, J. Liu, B. Sun, H. Chu, J. Shen, Acta Mater. 165 (2019) 444–458.
- [148] Z. Fu, B.E. MacDonald, Z. Li, Z. Jiang, W. Chen, Y. Zhou, E.J. Lavernia, Mater. Res. Lett. 6 (2018) 634–640.
- [149] P. Shi, R. Li, Y. Li, Y. Wen, Y. Zhong, W. Ren, Z. Shen, T. Zheng, J. Peng, X. Liang, Science 373 (2021) 912–918.
- [150] D. Miracle, J. Miller, O. Senkov, C. Woodward, M. Uchic, J. Tiley, Entropy 16 (2014) 494–525.
- [151] M.C. Troparevsky, J.R. Morris, P.R. Kent, A.R. Lupini, G.M. Stocks, Phys. Rev. X 5 (2015) 011041.
- [152] J.W. Yeh, JOM 65 (2013) 1759–1771.
- [153] S. Wei, F. He, C.C. Tasan, J. Mater. Res. 33 (2018) 2924-2937.
- [154] R. Wang, Y. Tang, S. Li, H. Zhang, Y. Ye, L.A. Zhu, Y. Ai, S. Bai, Mater. Des. 162 (2019) 256–262.
- [155] D. Li, Z. Li, L. Xie, Y. Zhang, W. Wang, Nano Res. 15 (2021) 4859-4866.

- [156] C.C. Tasan, M. Diehl, D. Yan, M. Bechtold, F. Roters, L. Schemmann, C. Zheng, N. Peranio, D. Ponge, M. Koyama, K. Tsuzaki, D. Raabe, Ann. Rev. Mater. Res. 45 (2015) 391–431.
- [157] S. Wei, S.J. Kim, J. Kang, Y. Zhang, Y. Zhang, T. Furuhara, E.S. Park, C.C. Tasan, Nat. Mater. 19 (2020) 1175–1181.
- [158] H. Jiang, D. Qiao, W. Jiao, K. Han, Y. Lu, P.K. Liaw, J. Mater. Sci. Technol. 61 (2021) 119–124.
- [159] M. Wang, Y. Lu, T. Wang, C. Zhang, Z. Cao, T. Li, P.K. Liaw, Scr. Mater. 204 (2021) 114132.
- [160] J.M. Torralba, P. Alvaredo, A. García-Junceda, Powder Metall. 62 (2019) 84-114.
- [161] J.M. Torralba, P. Alvaredo, A. García-Junceda, Powder Metall. 63 (2020) 227–236.
- [162] A.O. Moghaddam, N.A. Shaburova, M.N. Samodurova, A. Abdollahzadeh, E.A. Trofimov, J. Mater. Sci. Technol. 77 (2021) 131–162.
 [163] J. Ren, Y. Zhang, D. Zhao, Y. Chen, S. Guan, Y. Liu, L. Liu, S. Peng, F. Kong,
- [163] J. Ren, Y. Zhang, D. Zhao, Y. Chen, S. Guan, Y. Liu, L. Liu, S. Peng, F. Kong, J.D. Poplawsky, Nature 608 (2022) 62–68.
- [164] Z. Sun, X. Tan, C. Wang, M. Descoins, D. Mangelinck, S.B. Tor, E.A. Jägle, S. Zaefferer, D. Raabe, Acta Mater. 204 (2021) 116505.
 [165] J.M. Park, J. Choe, J.G. Kim, J.W. Bae, J. Moon, S. Yang, K.T. Kim, J.H. Yu,
- H.S. Kim, Mater. Res. Lett. 8 (2020) 1–7.
- [166] D. Lin, L. Xu, H. Jing, Y. Han, L. Zhao, F. Minami, Addit. Manuf. 32 (2020) 101058.
- [167] L. He, S. Wu, A. Dong, H. Tang, D. Du, G. Zhu, B. Sun, W. Yan, J. Mater. Sci. Technol. 117 (2022) 133–145.
- [168] M. Zhang, X. Zhou, D. Wang, L. He, X. Ye, W. Zhang, J. Alloy. Compd. 893 (2022) 162259.
 [169] B. Xiao, W. Jia, H. Tang, J. Wang, L. Zhou, J. Mater. Sci. Technol. 108 (2022)
- 54–63. [170] S. Cooke, K. Ahmadi, S. Willerth, R. Herring, J Manuf, Processes 57 (2020)
- 978–1003.
- [171] H. Liu, D. Yang, Q. Jiang, Y. Jiang, W. Yang, L. Liu, L.C. Zhang, J. Mater. Sci. Technol. 140 (2022) 79–120.
- [172] F. Haftlang, H.S. Kim, Mater. Des. 211 (2021) 110161.
- [173] J. Fu, H. Li, X. Song, M. Fu, J. Mater. Sci. Technol. 122 (2022) 165-199.
- [174] Y. Peng, C. Jia, L. Song, Y. Bian, H. Tang, G. Cai, G. Zhong, Intermetallics 145 (2022) 107557.
- [175] Z. Fu, B. Yang, K. Gan, D. Yan, Z. Li, G. Gou, H. Chen, Z. Wang, Corros. Sci. 190 (2021) 109695.
- [176] H. Khodashenas, H. Mirzadeh, J. Mater. Res. Technol. 21 (2022) 3795-3814.
- [177] Y. Lu, X. Wu, Z. Fu, Q. Yang, Y. Zhang, Q. Liu, T. Li, Y. Tian, H. Tan, Z. Li, J. Mater. Sci. Technol. 126 (2022) 15–21.
- [178] W.C. Lin, Y.-J. Chang, T.-H. Hsu, S. Gorsse, F. Sun, T. Furuhara, A.C. Yeh, Addit. Manuf. 36 (2020) 101601.
- [179] F. Otto, A. Dlouhý, C. Somsen, H. Bei, G. Eggeler, E.P. George, Acta Mater. 61 (2013) 5743–5755.
- [180] K.V.S. Thurston, B. Gludovatz, A. Hohenwarter, G. Laplanche, E.P. George, R.O. Ritchie, Intermetallics 88 (2017) 65–72.
- [181] Z. Wu, H. Bei, G.M. Pharr, E.P. George, Acta Mater. 81 (2014) 428–441.
- [182] Z. Zhang, H. Sheng, Z. Wang, B. Gludovatz, Z. Zhang, E.P. George, Q. Yu, S.X. Mao, R.O. Ritchie, Nat. Commun. 8 (2017) 14390.
- [183] Q. Ding, X. Fu, D. Chen, H. Bei, B. Gludovatz, J. Li, Z. Zhang, E.P. George, Q. Yu, T. Zhu, Mater. Today 25 (2019) 21–27.
- [184] A. Haglund, M. Koehler, D. Catoor, E.P. George, V. Keppens, Intermetallics 58 (2015) 62–64.
- [185] D.T. Pierce, J.A. Jiménez, J. Bentley, D. Raabe, J.E. Wittig, Acta Mater. 100 (2015) 178–190.
- [186] G. Laplanche, P. Gadaud, O. Horst, F. Otto, G. Eggeler, E.P. George, J. Alloy. Compd. 623 (2015) 348–353.
- [187] Z. Zhang, M.M. Mao, J. Wang, B. Gludovatz, Z. Zhang, S.X. Mao, E.P. George, Q. Yu, R.O. Ritchie, Nat. Commun. 6 (2015) 10143.
- [188] S. Huang, W. Li, S. Lu, F. Tian, J. Shen, E. Holmström, L. Vitos, Scr. Mater. 108 (2015) 44–47.
- [189] Z. Qiu, C. Yao, K. Feng, Z. Li, P.K. Chu, Int. J. Lightweight Mater. Manuf. 1 (2018) 33–39.
- [190] J. Liu, X. Guo, Q. Lin, Z. He, X. An, L. Li, P.K. Liaw, X. Liao, L. Yu, J. Lin, Sci. China Mater. 62 (2019) 853–863.
- [191] P. Shi, W. Ren, T. Zheng, Z. Ren, X. Hou, J. Peng, P. Hu, Y. Gao, Y. Zhong, P.K. Liaw, Nat. Commun. 10 (2019) 489.